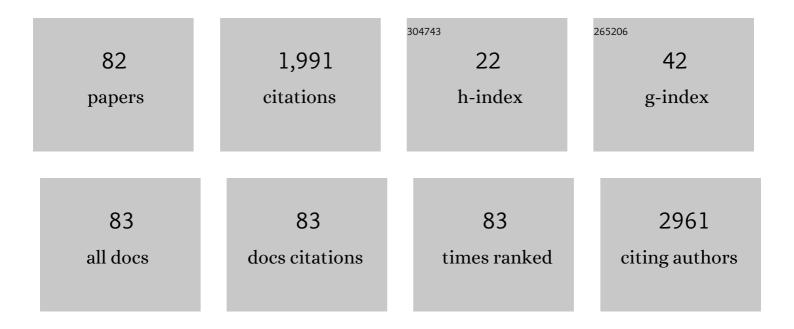
## Tamotsu Zako

List of Publications by Year in descending order

Source: https://exaly.com/author-pdf/1008231/publications.pdf Version: 2024-02-01



#	Article	IF	CITATIONS
1	Recent advances in research on biointerfaces: From cell surfaces to artificial interfaces. Journal of Bioscience and Bioengineering, 2022, , .	2.2	6
2	Insulin-derived amyloidosis (insulin ball) and skin-related complications of insulin therapy. Proceedings for Annual Meeting of the Japanese Pharmacological Society, 2022, 95, 3-S34-3.	0.0	0
3	Colorimetric detection of thrombin based on signal amplification by transcription-reverse transcription concerted reaction using non-crosslinking aggregation of gold nanoparticles. Analytical Sciences, 2022, 38, 3-7.	1.6	5
4	Differences in interaction lead to the formation of different types of insulin amyloid. Scientific Reports, 2022, 12, .	3.3	4
5	Insulin amyloid fibrils interact directly with the NLRP3, resulting in inflammasome activation and pyroptotic cell death. International Journal of Immunopathology and Pharmacology, 2021, 35, 205873842110383.	2.1	4
6	Molecular detection using aptamer-modified gold nanoparticles with an immobilized DNA brush for the prevention of non-specific aggregation. RSC Advances, 2021, 11, 11984-11991.	3.6	10
7	Protein-Functionalized Gold Nanoparticles for Antibody Detection Using the Darkfield Microscopic Observation of Nanoparticle Aggregation. Analytical Sciences, 2021, 37, 507-511.	1.6	8
8	Degradation of insulin amyloid by antibiotic minocycline and formation of toxic intermediates. Scientific Reports, 2021, 11, 6857.	3.3	9
9	Transcription-Based Amplified Colorimetric Thrombin Sensor Using Non-Crosslinking Aggregation of DNA-Modified Gold Nanoparticles. Sensors, 2021, 21, 4318.	3.8	9
10	Inhibition of amyloid formation of amyloid β (1–42), amylin and insulin by 1,5-diazacyclooctanes, a spermine-acrolein conjugate. Bioorganic and Medicinal Chemistry, 2021, 46, 116391.	3.0	3
11	Signal-amplified Colorimetric Biosensors Using Gold Nanoparticles. Bunseki Kagaku, 2021, 70, 661-670.	0.2	1
12	Insulinâ€derived amyloidosis without a palpable mass at the insulin injection site: A report of two cases. Journal of Diabetes Investigation, 2020, 11, 1002-1005.	2.4	18
13	Insulin amyloid polymorphs: implications for iatrogenic cytotoxicity. RSC Advances, 2020, 10, 37721-37727.	3.6	12
14	Clinical and MRI characteristics and follow-up studies of insulin-derived amyloidosis. Amyloid: the International Journal of Experimental and Clinical Investigation: the Official Journal of the International Society of Amyloidosis, 2019, 26, 156-157.	3.0	4
15	Toxicity of insulin-derived amyloidosis: a case report. BMC Endocrine Disorders, 2019, 19, 61.	2.2	40
16	Detection of Gold Nanoparticles Aggregation Using Light Scattering for Molecular Sensing. Analytical Sciences, 2019, 35, 685-690.	1.6	16
17	Molecular chaperone prefoldin-assisted biosynthesis of gold nanoparticles with improved size distribution and dispersion. Biomaterials Science, 2019, 7, 1801-1804.	5.4	5
18	Analysis of the degradation of amyloid beta fibrils after separation via the combination of nonâ€denaturing agarose electrophoresis and Congo red dye staining. Separation Science Plus, 2019, 2, 322-328.	0.6	3

Тамотѕи Ζако

#	Article	IF	CITATIONS
19	Construction of Quenchbodies to detect and image amyloid β oligomers. Analytical Biochemistry, 2018, 550, 61-67.	2.4	15
20	Prefoldin, a jellyfish-like molecular chaperone: functional cooperation with a group II chaperonin and beyond. Biophysical Reviews, 2018, 10, 339-345.	3.2	25
21	IAPP/amylin deposition, which is correlated with expressions of ASC and IL-1β in β-cells of Langerhans' islets, directly initiates NLRP3 inflammasome activation. International Journal of Immunopathology and Pharmacology, 2018, 32, 205873841878874.	2.1	23
22	Dark field microscopic analysis of discrete Au nanostructures: Understanding the correlation of scattering with stoichiometry. Chemical Physics Letters, 2017, 684, 310-315.	2.6	6
23	Contribution of the C-Terminal Region of a Group II Chaperonin to its Interaction with Prefoldin and Substrate Transfer. Journal of Molecular Biology, 2016, 428, 2405-2417.	4.2	9
24	Amorphous protein aggregation monitored using fluorescence selfâ€quenching. FEBS Letters, 2016, 590, 3501-3509.	2.8	15
25	Dark Field Microscopic Sensitive Detection of Amyloid Fibrils Using Gold Nanoparticles Modified with Antibody. Analytical Sciences, 2016, 32, 307-311.	1.6	12
26	Inhibition of Amyloid β Protein Fibrillation via Carboxypeptidase Y after Protein Trapping Using Immunoaffinity Membranes. Chemistry Letters, 2016, 45, 1241-1243.	1.3	3
27	1,5â€Diazacyclooctanes, as Exclusive Oxidative Polyamine Metabolites, Inhibit Amyloidâ€≺i>β(1â€40) Fibrillization. Advanced Science, 2016, 3, 1600082.	11.2	16
28	Oxidative Stress: 1,5-Diazacyclooctanes, as Exclusive Oxidative Polyamine Metabolites, Inhibit Amyloid-β (1-40) Fibrillization (Adv. Sci. 10/2016). Advanced Science, 2016, 3, .	11.2	0
29	Extra-luminal detection of assumed colonic tumor site by near-infrared laparoscopy. Surgical Endoscopy and Other Interventional Techniques, 2016, 30, 4153-4159.	2.4	11
30	Adsorption and separation of amyloid beta aggregates using ferromagnetic nanoparticles coated with charged polymer brushes. Journal of Materials Chemistry B, 2015, 3, 3351-3357.	5.8	7
31	NADH oxidase and alkyl hydroperoxide reductase subunit C (peroxiredoxin) from <i>Amphibacillus xylanus</i> form an oligomeric assembly. FEBS Open Bio, 2015, 5, 124-131.	2.3	6
32	Cancer-targeted near infrared imaging using rare earth ion-doped ceramic nanoparticles. Biomaterials Science, 2015, 3, 59-64.	5.4	46
33	Cysteine inhibits amyloid fibrillation of lysozyme and directs the formation of small wormâ€like aggregates through nonâ€covalent interactions. Biotechnology Progress, 2014, 30, 470-478.	2.6	17
34	Degeneration of amyloid-ß fibrils caused by exposure to low-temperature atmospheric-pressure plasma in aqueous solution. Applied Physics Letters, 2014, 104, .	3.3	18
35	Cysteine inhibits the fibrillisation and cytotoxicity of amyloid- $\hat{1}^2$ 40 and 42: implications for the contribution of the thiophilic interaction. Physical Chemistry Chemical Physics, 2014, 16, 3566.	2.8	10
36	Application of biomaterials for the detection of amyloid aggregates. Biomaterials Science, 2014, 2, 951-955.	5.4	12

Тамотѕи Ζако

#	Article	IF	CITATIONS
37	Detection of DNA induced gold nanoparticle aggregation with dark field imaging. Chemical Communications, 2013, 49, 7531.	4.1	35
38	Formation of non-toxic Al <sup>2</sup> fibrils by small heat shock protein under heat-stress conditions. Biochemical and Biophysical Research Communications, 2013, 430, 1259-1264.	2.1	5
39	Rapid Surface–Biostructure Interaction Analysis Using Strong Metal-Based Nanomagnets. Langmuir, 2013, 29, 14117-14123.	3.5	2
40	Human Prefoldin Inhibits Amyloid-β (Aβ) Fibrillation and Contributes to Formation of Nontoxic Aβ Aggregates. Biochemistry, 2013, 52, 3532-3542.	2.5	43
41	Prefoldin Protects Neuronal Cells from Polyglutamine Toxicity by Preventing Aggregation Formation. Journal of Biological Chemistry, 2013, 288, 19958-19972.	3.4	49
42	A Structure-Toxicity Study of Aß42 Reveals a New Anti-Parallel Aggregation Pathway. PLoS ONE, 2013, 8, e80262.	2.5	41
43	Nanoscopic and Photonic Ultrastructural Characterization of Two Distinct Insulin Amyloid States. International Journal of Molecular Sciences, 2012, 13, 1461-1480.	4.1	10
44	Naked-eye Detection of Amyloid Aggregates Using Gold Nanoparticles Modified with Amyloid Beta Antibody. Analytical Sciences, 2012, 28, 73-76.	1.6	18
45	DNA-Templating Mass Production of Gold Trimer Rings for Optical Metamaterials. Journal of Physical Chemistry C, 2012, 116, 15028-15033.	3.1	21
46	Amyloid oligomer detection by immobilized molecular chaperone. Biochemical Engineering Journal, 2012, 61, 28-33.	3.6	6
47	Cell Interaction Study of Amyloid by Using Luminescent Conjugated Polythiophene: Implication that Amyloid Cytotoxicity Is Correlated with Prolonged Cellular Binding. ChemBioChem, 2012, 13, 358-363.	2.6	12
48	2C1524 Newly developed photon counting histogram method for amyloid beta oligomer formation(Protein: Function 1,The 48th Annual Meeting of the Biophysical Society of Japan). Seibutsu Butsuri, 2011, 51, S79.	0.1	0
49	Immobilized Insulin Amyloid Enhances Cell Adhesion and Proliferation Due to Interaction with Fibronectin. Chemistry Letters, 2011, 40, 315-317.	1.3	2
50	Nuclear Exportin Receptor CAS Regulates the NPI-1–Mediated Nuclear Import of HIV-1 Vpr. PLoS ONE, 2011, 6, e27815.	2.5	19
51	1P085 Amyloid beta oligomer studied by photon counting histogram(Protein:Function,The 48th Annual) Tj ETQq1	1 0.7843 0.1	314 rgBT /0
52	Size-selective recognition of gold nanoparticles by a molecular chaperone. Chemical Physics Letters, 2010, 501, 108-112.	2.6	8
53	Amyloid oligomers. FEBS Journal, 2010, 277, 1347-1347.	4.7	2
54	Amyloid oligomers: formation and toxicity of $A\hat{I}^2$ oligomers. FEBS Journal, 2010, 277, 1348-1358.	4.7	508

Тамотѕи Zako

#	Article	IF	CITATIONS
55	Thermodynamic Characterization of the Interaction between Prefoldin and Group II Chaperonin. Journal of Molecular Biology, 2010, 399, 628-636.	4.2	16
56	Hyperthermophilic archaeal prefoldin shows refolding activity at low temperature. Biochemical and Biophysical Research Communications, 2010, 391, 467-470.	2.1	7
57	A facile method towards cyclic assembly of gold nanoparticles using DNA template alone. Chemical Communications, 2010, 46, 6132.	4.1	24
58	Bio-supramolecular photochirogenesis with molecular chaperone: enantiodifferentiating photocyclodimerization of 2-anthracenecarboxylate mediated by prefoldin. Photochemical and Photobiological Sciences, 2010, 9, 655-660.	2.9	21
59	Cyclic RGD peptide-labeled upconversion nanophosphors for tumor cell-targeted imaging. Biochemical and Biophysical Research Communications, 2009, 381, 54-58.	2.1	104
60	Bovine Insulin Filaments Induced by Reducing Disulfide Bonds Show a Different Morphology, Secondary Structure, and Cell Toxicity from Intact Insulin Amyloid Fibrils. Biophysical Journal, 2009, 96, 3331-3340.	0.5	111
61	Dynamics of group II chaperonin and prefoldin probed by <sup>13</sup> C NMR spectroscopy. Proteins: Structure, Function and Bioinformatics, 2008, 70, 1257-1263.	2.6	8
62	Improvement of dispersion stability and characterization of upconversion nanophosphors covalently modified with PEG as a fluorescence bioimaging probe. Journal of Materials Science, 2008, 43, 5325-5330.	3.7	47
63	Formation of highly toxic soluble amyloid beta oligomers by the molecular chaperone prefoldin. FEBS Journal, 2008, 275, 5982-5993.	4.7	55
64	Measuring Adsorption of a Hydrophobic Probe with a Surface Plasmon Resonance Sensor to Monitor Conformational Changes in Immobilized Proteins. Biotechnology Progress, 2008, 19, 1348-1354.	2.6	19
65	Effect of the C-terminal Truncation on the Functional Cycle of Chaperonin GroEL. Journal of Biological Chemistry, 2008, 283, 23931-23939.	3.4	30
66	3P-033 Analysis of Ab oligomer formation by photon counting histogram (PCH) and fluorescence correlation spectroscopy (FCS)(The 46th Annual Meeting of the Biophysical Society of Japan). Seibutsu Butsuri, 2008, 48, S132.	0.1	0
67	Selectivity improvement in protein nanopatterning with a hydroxy-terminated self-assembled monolayer template. Nanotechnology, 2007, 18, 305304.	2.6	16
68	3P314 Single-molecule analysis of the complex formed between molecular chaperone prefoldin and amyloid beta(Bioimaging,Poster Presentations). Seibutsu Butsuri, 2007, 47, S281.	0.1	0
69	Complex formation of CdSe/ZnS/TOPO nanocrystal vs. molecular chaperone in aqueous solution by hydrophobic interaction. Journal of Luminescence, 2007, 127, 192-197.	3.1	6
70	Localization of Prefoldin Interaction Sites in the Hyperthermophilic Group II Chaperonin and Correlations between Binding Rate and Protein Transfer Rate. Journal of Molecular Biology, 2006, 364, 110-120.	4.2	42
71	2P103 Characterization of flexible insulin fibrils induced by reducing agent(31. Protein folding and) Tj ETQq1 1 C 2006, 46, S321.	).784314 0.1	rgBT /Overloo 0
72	Contribution of the C-terminal region to the thermostability of the archaeal group II chaperonin from Thermococcus sp. strain KS-1. Extremophiles, 2006, 10, 451-459.	2.3	20

Ταμοτςυ Ζακο

#	Article	IF	CITATIONS
73	Characterization of Archaeal Group II Chaperonin-ADP-Metal Fluoride Complexes. Journal of Biological Chemistry, 2005, 280, 40375-40383.	3.4	29
74	Interaction of a Small Heat Shock Protein of the Fission Yeast, Schizosaccharomyces pombe, with a Denatured Protein at Elevated Temperature. Journal of Biological Chemistry, 2005, 280, 32586-32593.	3.4	19
75	Micropatterning Oligonucleotides on Single-Crystal Diamond Surface by Photolithography. Japanese Journal of Applied Physics, 2005, 44, L295-L298.	1.5	8
76	Facilitated release of substrate protein from prefoldin by chaperonin. FEBS Letters, 2005, 579, 3718-3724.	2.8	44
77	The role of firefly luciferase C-terminal domain in efficient coupling of adenylation and oxidative steps. FEBS Letters, 2005, 579, 4389-4394.	2.8	22
78	Role of the Helical Protrusion in the Conformational Change and Molecular Chaperone Activity of the Archaeal Group II Chaperonin. Journal of Biological Chemistry, 2004, 279, 18834-18839.	3.4	41
79	Kinetics and Binding Sites for Interaction of the Prefoldin with a Group II Chaperonin. Journal of Biological Chemistry, 2004, 279, 31788-31795.	3.4	53
80	The immobilization of DNA on microstructured patterns fabricated by maskless lithography. Sensors and Actuators B: Chemical, 2004, 97, 243-248.	7.8	29
81	Preferential immobilization of biomolecules on silicon microstructure array by means of electron beam lithography on organosilane self-assembled monolayer resist. Applied Surface Science, 2004, 234, 102-106.	6.1	24
82	Refolding of Firefly Luciferase Immobilized on Agarose Beads. Journal of Biochemistry, 2000, 127, 351-354.	1.7	7